Impedance Margin Ratio: a New Metric for Small-Signal System Strength

Yue Zhu, *Member, IEEE*, Timothy C. Green, *Fellow, IEEE*, Xiaoyao Zhou,Yitong Li, *Member, IEEE*, Dechao Kong, Yunjie Gu, *Senior Member, IEEE*

***Abstract*—The high and growing penetration of inverter-based resources (IBR) in power systems challenges the way that system strength is assessed. It has been noticed that the standard indicator of system strength, short-circuit ratio (SCR), is not fully effective in anticipating the sub/super-synchronous oscillation phenomena that can arise from interactions of the control system of an IBR and the rest of the system. In this paper, system strength is first viewed from two perspectives, small-signal system strength and large-signal system strength, which is a natural separation considering the markedly different response of an IBR in normal operation and under faults. For assessing the onset of small-signal instability, a new metric for small-signal system strength is proposed and named Impedance Margin Ratio (IMR). IMR is the ratio between the allowed variation of the impedance of an IBR and the original value of the impedance at a particular point of interconnection. IMR is assessed at the oscillatory frequency of the dominant mode or taken as the minimum value across several modes. It is shown that as a localised frequency-domain indicator, IMR can successfully reveal weak points in the system towards various causes of oscillations.**

***Index Terms*—Grid strength, small-signal system strength, inverter-based resource, short-circuit ratio, sub-synchronous oscillation, impedance margin ratio**

I. Introduction

Power systems worldwide are transforming from systems dominated by synchronous generators (SGs) to ones where inverter-based resources (IBRs) become dominant [1]–[3], in the drive to meet the decarbonisation targets. One consequence of the displacement of SGs by IBRs is that system strength is decreasing in some regions [4]. Traditionally, short-circuit ratio (SCR) is the standard measure of system strength and it is used for indicating the ability of a system to accommodate connection to a new apparatus at a particular point of interconnection (POI) [5], [6]. In its simple form, SCR is assessed by performing a three-phase fault analysis at a specific POI prior to the connection of the new apparatus at that POI. The ratio of the short-circuit capacity and the nominal power of the apparatus at that POI is defined as SCR. The SCR such defined is equivalent to the reciprocal of the Thévenin impedance seen at the POI in a per-unit value normalised to the rating of the apparatus being connected. A large SCR indicates that the system can provide a large amount of current into the fault location and carries an implication that the system is able to hold the system voltage close to the nominal value in the face of perturbations and that the POI has a low series Thévenin impedance. The wide application of SCR has led to system strength and SCR being sometimes used in an interchangeable fashion, i.e., a 'weak' system means a low SCR, and vice versa [7].

As SGs are gradually replaced by IBRs, using SCR as a sole definition for system strength leads to several drawbacks. First, SCR is based on a dichotomous view that voltage sources enhance system strength and other IBRs consume system strength, disregarding the fact that IBRs can be controlled to have system-supporting behaviours and potentially enhance system strength. Second, SCR is a static index that only considers impedance at the fundamental frequency, but IBRs may have much wider control bandwidths and interaction frequencies. Third, SCR is an index for strength assessment of a single-infeed system, i.e., it considers a single IBR connecting to the power system [8], [9]. If SCR at multiple locations are to be assessed, apparatus at these locations should all be treated as disconnected. As a result, SCR does not reflect the interaction among multiple IBRs in a multi-infeed system. Fourth, IBRs may saturate their currents during faults so the SCR calculated via fault analysis may diverge from the system strength under normal operation. For these reasons, it is no longer appropriate to use solely SCR as an all-purpose indicator of system strength or use SCR and system strength interchangeably amid the changing landscape where IBRs are becoming increasingly dominant.

Researchers and system operators around the world have revisited the definition of system strength in recent years [6], [10], [11]. It is underscored in [6] that system strength encompasses a broad range of issues and their implications on power system operability, and refers to the ability of system equipment to operate in a stable manner and to tolerate perturbations occurring within the connected devices. It is stated in [10] that system strength is a characteristic of power systems that relates to the size of the change in voltage following a fault or disturbance. [11] further classified system strength into steady-state system strength and dynamic-state system strength, subject to system behaviours towards small and large disturbances in the system. These reconsiderations of system strength have prompted researchers to seek new system strength metrics to better describe the relevant characteristics. Some variants of SCR have been proposed lately to overcome the shortcoming that SCR can only be used for connection

This work was supported by National Grid ESO under the Network Innovation Allowance (NIA) Project NIA2_NGESO020. (*Corresponding Author: Yue Zhu*).

Yue Zhu, Timothy C. Green, and Yunjie Gu are with the Department of Electrical and Electronic Engineering, Imperial College London, SW7 2BX, London, UK (e-mail: yue.zhu18@imperial.ac.uk; t.green@imperial.ac.uk; yunjie.gu@imperial.ac.uk).

Xiaoyao Zhou is with National Grid ESO, CV34 6DA, Warwick, UK (e-mail: Xiaoyao.Zhou@nationalgrideso.com).

Yitong Li is with the School of Electrical Engineering, Xi'an Jiaotong University, 710049, Xi'an, China (e-mail: yitongli@xjtu.edu.cn).

Dechao Kong was with National Grid ESO (2020-2023), CV34 6DA, Warwick, UK (e-mail: Dechao.kong.dipsi20@said.oxford.edu).

of a single IBR. For example, composite short-circuit ratio (CSCR) [12] and weighted short-circuit ratio (WSCR) [13] are proposed as aggregated metrics for system strength when a group of IBRs is going to connect to the same high-voltage bus. However, both CSCR and WSCR omit the potential for interaction among the newly connected IBRs. Equivalent circuit short circuit ratio (ESCR) is further proposed [5] for assessing the interaction among IBRs by applying an interaction factor, which is defined by introducing a small voltage change at one POI and observing the small change of bus voltage at another POI. In [9], a generalised short circuit ratio (gSCR) has been proposed to reflect the interaction of IBRs in a multi-infeed system, which is an overall metric for the entire system by considering static voltage stability. While discussions on the relative merits of these new definitions are still ongoing, all of these new metrics are defined through quantities assessed at the fundamental frequency which means that it is difficult to reflect the oscillation behaviours in wider frequencies.

To address the wide frequency interactions, [14] extends SCR from a fundamental-frequency quantity to a frequency-domain spectrum. [15] combines the frequency-domain approach with gSCR for multi-infeed systems. [16] further accommodates heterogeneous IBRs into gSCR by using the whole-system impedance/admittance matrix [17] to take into account the detailed control of all apparatuses and their interactions in the system. The investigation down this line has made significant progress but there are still propelling questions yet to be answered. It is not clear which points in the frequency spectrum are of importance. Furthermore, there are no specific criteria or rules of thumb indicating the acceptable threshold of the newly defined system strengths. The multi-infeed analysis based on gSCR is essentially a worst-case analysis for the voltage stiffness of the entire system but is not clear how gSCR can be related back to a particular POI.

It is clear that there is not a good overall indicator for all aspects of system strength. Therefore, this paper first draws a distinction between system strength in two perspectives: small-signal system strength and large-signal system strength, to reflect the distinctly different responses of IBR towards small and large disturbances. A new metric, named impedance margin ratio (IMR), is then proposed to serve as an indicator specifically for small-signal system strength. The definition of IMR is the ratio of the maximum allowed variation of the IBR impedance at the POI to the original value of impedance where the allowed variation is set to avoid a movement of an oscillatory mode to the right-half plane (RHP). This new metric processes the following merits:

1) IMR is analysed in the frequency domain, especially at the oscillatory frequency of a mode of concern. IMR points to an observable poorly damped oscillatory mode at the POI with a specific stability margin.
2) IMR is a localised value indicating the small-signal system strength at the POI being considered and hence it can be used to pinpoint weak areas in the system.
3) IMR is calculated from the whole-system admittance model which naturally reflects the interactions among multiple apparatuses in a multi-infeed system.

This paper is organised as follows. Small-signal and large-signal system strength is classified in Section II. In section III, IMR is introduced with its key properties illustrated. In Section IV, the relationship of IMR with SCR and its variants are discussed. Section V describes detailed instructions for practical implementations. A 4-bus system and a modified IEEE 68-bus are then employed in Section VI as case studies to validate the application of IMR in different scales of work, proving its effectiveness and practicability. The last section concludes the paper.

II. Distinction of System Strengths

As highlighted in the introduction, there is a need to make a distinction between system strength in normal operation and under faults. To this end, we define small-signal and large-signal system strengths here, as set out in Table I and the features of each will now be discussed.

Small-signal system strength considers the dynamic and possibly oscillatory behaviour of system voltage in response to small perturbations around the operating point which is an example of the general topic of small-signal systems analysis. Using frequency domain modelling, the detailed control behaviour of IBRs and their interactions in wide frequencies can be represented but this applies only to linearisation around given operating points. Because the voltage at each POI is essentially a state of the system, the dynamic behaviour of voltage will be dependent on the system eigenvalues, and especially, the conjugate complex pairs with real-part close to zero. These eigenvalues will shape the oscillatory behaviour of the voltage towards small perturbations in magnitude, frequency and settling time. Therefore, a potential solution for assessing the small-signal system strength is through the eigenvalue analysis. Although the state-space model is the most straightforward way to illustrate the small-signal behaviour, it is worth noting that such a model is a white-box model requiring full knowledge of the system, including the detailed design of the IBR, which is usually not available to system operators. Alternatively, an impedance model, which is a black-box model, turns out to be a favourable solution for assessing small-signal strength for systems with high penetration of IBRs [14]–[16]. Another benefit of using impedance model is that it represents the connected device as a one-port network by describing the voltage and current at its port. This configuration aggregates the influence from all the internal states and parameters of the IBR, so that a single value can be found to represent the strength at the POI. The expected use of a small-signal system strength metric is to address the potential instability and oscillations caused by IBR interactions, especially where strong control coupling is induced in a weak grid due to long transmission lines and/or inadequate voltage regulation.

The large-signal system strength concerns the contribution towards fault currents to trigger protection actions and the recovery of a bus voltage following large disturbances such as a local three-phase fault or a deep voltage dip caused by a remote fault. Such analysis is carried out via short-circuit analysis at various locations. Although the short-circuit

TABLE I
DISTINCTIONS OF TWO TYPES OF SYSTEM STRENGTH METRICS

	Metrics for small-signal system strength	**Metrics for large-signal system strength**
Features	• Small perturbations around an operation point • Frequency-domain analysis • Linear system stability analysis • Small-signal models of IBRs are integrated	• Large perturbations like faults • Fundamental frequency analysis • Nonlinear system when IBRs are present • Proper models of IBRs for short-circuit analysis are absent
Intended indications	• Inadequate voltage regulation • Potential weak-grid oscillations and voltage collapse • Small-signal interactions among inverters and grid	• Low fault current or false fault current injection • Maloperation of protection • Excessive recovery time from voltage dips • Risk of fault-induced voltage collapse
Metrics	• Frequency-domain impedance and its variants	• Normalised fault current

response may contain rich frequency components, it is difficult and usually unnecessary to consider all of them and fundamental frequency analysis is considered sufficient. Subject to a large perturbation, the IBR present may exhibit nonlinear behaviour because of the operation of their internal saturation control against, for example, over-current. So far, efforts to develop an appropriate IBR model to describe nonlinear behaviour and fault contribution in a way amenable to analysis are still ongoing. IBRs are often approximated as a voltage source in series with an equivalent reactance of 1 p.u. to represent fault current contribution saturated to the nominal current, or simply an open circuit with no fault contribution at all [5]. Such approximations are very inaccurate, often yielding underestimated fault currents. An iterative fault calculation scheme is presented in [18] for a more accurate fault current modelling considering authentic current saturation control of IBRs. The expected uses of large-signal system strength metrics are to identify risks of low fault current and maloperation of protection. The same metrics may also prove useful to warn against fault-induced voltage collapse or excessive recovery time from voltage dips.

If only SGs are present in the system, the small-signal and large-signal system strengths are unified into SCR. That is, a normalised fault current is the reciprocal of the per-unit Thévenin impedance at the fundamental frequency. Therefore, the small-signal and large-signal system strengths defined above are consistent with each other.

III. Impedance Margin Ratio

A. Preliminaries

The definition of IMR has been created based on a previous study of the whole-system admittance model and impedance participation factor [19], [20], so these concepts are briefly reviewed first to facilitate reading.

1) Whole-system admittance model: A whole-system admittance model is essentially a frequency-domain admittance matrix to describe the dynamic characteristics of the entire system. It is a small-signal model which selects the bus voltage at each POI as system input, and the current flow from the apparatus to the bus as system output, thus the system becomes a multi-input and multi-output system. To represent such a system, we can introduce virtual small-signal voltage perturbations $\tilde{v}$ in series with apparatuses at each POI as the input, and choose the corresponding small-signal current Δi perturbations as the output, as shown in Fig. 1. The whole-system admittance Y^{sys} is then defined as the transfer function matrix from the input to the output, i.e.,

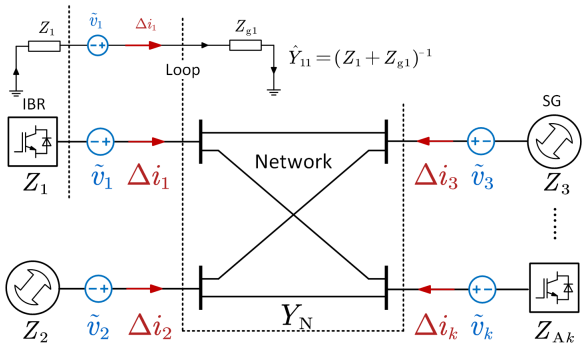


Fig. 1. Virtual small-signal voltage injection at each node to form Y^{sys}. [17] ©2022 IEEE.

$$Y^{\text{sys}} \cdot \tilde{v} = \Delta i, \tag{1}$$

where $\tilde{v} = [\tilde{v}_1, \tilde{v}_2, \cdots, \tilde{v}_n]^\top$ and $\Delta i = [\Delta i_1, \Delta i_2, \cdots, \Delta i_n]^\top$, and n is the total number of buses. It is worth mentioning that $\tilde{v}$ in Fig. 1 represents a group of additional perturbations added on the voltage at the POI, rather than the internal voltage sources from Thevenin equivalence of the apparatus. For an SG or a grid-forming inverter which is modelled as an internal voltage source in series with an impedance, or a grid-following inverter which is modelled as an internal current source in parallel with an impedance, its internal source is considered to be in steady-state and hence zero for small-signal modelling. Consequently, for apparatus at bus-k, regardless of its type, is modelled solely as an impedance Z_{Ak}.

It was shown in [20] that through a feedback arrangement, Y^{sys} can be stated as

$$Y^{\text{sys}} = (I + Y_{\text{N}} Z_{\text{A}})^{-1} Y_{\text{N}}, \tag{2}$$

where Y_{N} is the conventional nodal admittance matrix consisting of admittance of branches but extended in frequency domain, Z_{A} is a diagonal impedance matrix where the diagonal entries are the impedances of apparatus at each POI, and I is the identity matrix. The elements of Y^{sys} are all transfer functions or impedance spectra, sharing a common set of poles

which are also identical to the eigenvalues of the state-space model, i.e., the criteria that the system maintains stable is that there are no RHP poles for each of the element in Y^{sys}.

It is noted that a diagonal element of Y^{sys}, such as Y_{11}^{sys} at bus-1, is the inverse of the impedance of local IBR in series with the impedance of the grid seen from bus-1, i.e.,

$$Y_{11}^{\text{sys}} = (Z_{\text{A1}} + Z_{\text{g1}})^{-1}. \tag{3}$$

2) Impedance Participation Factor: Oscillatory behaviour is dependent on the eigenvalue of the state-space matrix $\boldsymbol{A}$. For a physical system, an eigenvalue λ is either a real number or a pair of conjugate complex values. When λ is conjugate complex, i.e.,

$$\lambda = \sigma \pm j\omega, \lambda \in eig(\boldsymbol{A}), \tag{4}$$

it refers to an oscillatory mode in the system, where σ refers to the damping of the mode (the rate at which an oscillation is dampened) and ω is the oscillation frequency. When there is a mode with a small damping factor in the system, one expects to see long-lasting oscillations in the system following a small disturbance such as a small step change in the load. In general, a mode λ is a global small-signal system stability indicator; global in the sense that it is a property of the whole system including IBRs in combination with everything else in the grid. However, it is worth noting that for a mode λ, its sensitivities to changes at various POIs will be different. This means that a mode, even if a poorly damped mode, may not be easily excited by adding perturbations from certain POIs. Equivalently, the mode may not be observable from these POIs because the mode controllability and observability at a POI have been shown to be numerically the same [21]. In such a case, we can say that these POIs are relatively 'strong'. This fact implies the possibility of a localised metric of system strength at different locations corresponding to the global oscillatory mode.

Now consider a small change added to the impedance of an IBR connected at bus-k, i.e., $\Delta Z_{\text{A}k}$, and the rest of the system unchanged. This change can be caused by a small perturbation of a control parameter of the IBR, a variation of its operating point, or scaling up or down by connecting or disconnecting a portion of apparatus from a farm of apparatuses (e.g. a wind farm). The change $\Delta Z_{\text{A}k}$ will lead to a variation on the system eigenvalue λ, i.e., $\Delta\lambda$. If in a single-phase system where $Z_{\text{A}k}$ is a scalar transfer function, and within a small range around $s = \lambda$, $\Delta\lambda$ can be calculated as

$$\Delta\lambda = \frac{\partial\lambda}{\partial Z_{\text{A}k}(\lambda)} \cdot \Delta Z_{\text{A}k}(\lambda), \tag{5}$$

where $\frac{\partial\lambda}{\partial Z_{\text{A}k}(\lambda)}$ represents the sensitivity of λ to the impedance of the IBR at bus-k at $s = \lambda$. According to the discussion in [17], such sensitivity equals the negative of the residue of Y_{kk}^{sys} at its pole $s = \lambda$, i.e.,

$$\frac{\partial\lambda}{\partial Z_{\text{A}k}(\lambda)} = -\text{Res}_\lambda Y_{kk}^{\text{sys}}, \tag{6}$$

where $\text{Res}_\lambda Y_{kk}^{\text{sys}}$ is the residue of Y_{kk}^{sys} at $s = \lambda$. Substituting (6) into (5) yields

$$\Delta\lambda = -\text{Res}_\lambda Y_{kk}^{\text{sys}} \cdot \Delta Z_{\text{A}k}(\lambda). \tag{7}$$

In a more common scenario where d-q synchronous frame is employed and $\Delta Z_{\text{A}k}(\lambda)$ and Y_{kk}^{sys} are 2×2 square matrices, (7) can be modified as

$$\Delta\lambda = \langle -\text{Res}_\lambda^* Y_{kk}^{\text{sys}}, \Delta Z_{\text{A}k} \rangle, \tag{8}$$

where $\text{Res}_\lambda^* Y_{kk}^{\text{sys}}$ is the conjugate transpose of the matrix of residues of Y_{kk}^{sys} at $s = \lambda$, and $\langle \cdot, \cdot \rangle$ denotes the Frobenius inner product of the two matrices. The detailed proof of (8) is given in [17]. It follows from (8) that $\text{Res}_\lambda^* Y_{kk}^{\text{sys}}$ quantifies how the perturbation of impedances yields the perturbation of eigenvalues and therefore is called impedance participation factor.

B. Definition

We now give a formal definition of IMR based on the impedance participation factor. If a strong correlation is found between $\Delta\lambda$ and $\Delta Z_{\text{A}k}$, it is more likely that λ will vary significantly for relatively small changes in the apparatus impedance and it is more likely that the mode will move to the RHP and become unstable as a result. Such a strong correlation means that the system is 'weak' seen from the location in question and with the IBR in question. In general, the direction of $\Delta Z_{\text{A}k}$ and the angle of $\Delta\lambda$ are both unknown. To keep λ in the left-half plane (stable) without knowing the angle of $\Delta\lambda$, we confine the magnitude of $\Delta\lambda$ to the absolute value of the real part of the existing mode, that is

$$|\Delta\lambda|_{\text{max}} = |\sigma|, \tag{9}$$

which we name a mode margin. Correspondingly, the change of impedance has a limitation on its magnitude, denoted by $\|\Delta Z_{\text{A}k}\|_{\text{max}}$. Since the angle of $\Delta Z_{\text{A}k}$ is unknown, we apply Cauchy inequality on (8) for worst-case estimation

$$|\Delta\lambda|_{\text{max}} = \left\|\text{Res}_\lambda^* Y_{kk}^{\text{sys}}\right\| \cdot \|\Delta Z_{\text{A}k}\|_{\text{max}} \tag{10}$$

where $\|\cdot\|$ denotes the Frobenius norm of a matrix. It follows from (9) and (10) that

$$\|\Delta Z_{\text{A}k}(\lambda)\|_{\text{max}} = \frac{|\sigma|}{\left\|\text{Res}_\lambda^* Y_{kk}^{\text{sys}}\right\|} \tag{11}$$

which we name the impedance margin. This is a conservative margin since a larger change might be allowed if $\Delta Z_{\text{A}k}$ were known to be in a safe direction, but the direction is considered arbitrary here. This is because the metric needs to be defined equitably at each POI, and the direction of impedance variation is usually unknown in practice.

IMR is then defined as the ratio between the impedance margin and the magnitude of the original impedance of the apparatus, i.e.,

$$\textbf{Impedance Margin Ratio (IMR)} \triangleq \frac{\|\Delta Z_{\text{A}k}(\lambda)\|_{\text{max}}}{\|Z_{\text{A}k}(\lambda)\|}. \tag{12}$$

Such a ratio is considered suitable for describing the small-signal system strength at a specific location: a large IMR means the system is tolerant to relatively large variations of the corresponding apparatus impedance in arbitrary directions, indicating a strong system; a small IMR indicates that a small change of apparatus condition (seen via its impedance) may

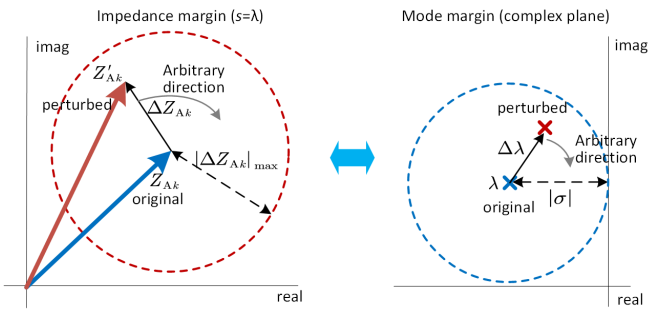


Fig. 2. IMR illustration on the complex plane.

easily shift the mode to the RHP and make the entire system unstable, which we can refer to as a weak system. For a fair comparison, the variation is scaled to the original impedance of the apparatus using a ratio representation. Combining (11) and (12) further yields

$$\mathbf{IMR} = \frac{|\sigma|}{\left\|\mathrm{Res}_{\lambda}^{*} Y_{kk}^{\mathrm{sys}}\right\| \left\|Z_{\mathrm{A}k}(\lambda)\right\|}. \tag{13}$$

Fig. 2 illustrates the principle of IMR on a complex plane. The left-hand part of the figure depicts the impedance margin of the apparatus at $s = \lambda$: the blue arrow is the original impedance vector, the red arrow represents the perturbed impedance $Z_{\mathrm{A}k}^{'} = Z_{\mathrm{A}k} + \Delta Z_{\mathrm{A}k}$. The right-hand part of the figure depicts the corresponding changes to the mode where the blue cross is the original oscillatory mode λ and the red cross is the new mode $\lambda+\Delta\lambda$ after the perturbation. The mode variation has a margin of $|\sigma|$, marked by the blue-dashed circle. As mentioned before, this is a conservative margin because the direction of $\Delta Z_{\mathrm{A}k}$ is considered arbitrary. In turn, the mode margin determines the impedance margin, marked by the red-dashed circle in the left-hand part. It can be seen from Fig. 2 that IMR is the ratio between the radius of the red-dashed circle and the length of the blue arrow (the magnitude of the original IBR impedance).

C. Properties

From the definition of IMR, several key properties follow, which reflect its essential benefits. They are introduced in this section and then discussed in detail.

Property 1. *IMR is a localised small-signal system strength metric. For a system with no RHP poles, IMR* $\in (0, +\infty)$. *The larger IMR is, the stronger the system is.*

This property follows directly from (13). IMR is calculated on a bus-by-bus basis. A large IMR indicates two things: first, the mode being examined does not already have a very low damping factor, and second, the mode is not highly sensitive to the impedance of the local apparatus. In such a case, the system is more tolerant to variations occurring in the device connected at the POI. Conversely, a small IMR refers to a poorly damped oscillatory mode observable at the POI, and a high risk that a perturbation of the impedance of the local apparatus could lead to the system becoming unstable, subject to the type and extent of the impedance change. It is yet not fully understood what exact value of IMR guarantees satisfactory system strength. Initial findings through case studies reveal that an IMR smaller than 0.5 indicates a weak system. By looking at IMR at different locations, system operators can quickly pinpoint the weak areas in the system.

Property 2. *IMR is an index for multi-infeed power systems and interactions among IBRs are naturally reflected in IMR.*

The key principle to distinguish a system strength metric for single- or multi-infeed power systems is whether it can reflect the interactions, especially the control interactions, among multiple IBRs at different locations. These interactions are of critical concern for system strength assessment because they can cause oscillations in the system [7]. Because such oscillations are small-signal phenomena, they essentially can be represented by oscillatory modes, which are also poles of the elements of Y^{sys}, as introduced in Section III-A1. In other words, interactions among IBRs can be represented by system oscillatory modes. For a mode λ which is caused by the control interaction among several IBRs, according to (8), the corresponding residue of Y_{kk}^{sys} at λ, $\mathrm{Res}_{\lambda}^{*} Y_{kk}^{\mathrm{sys}}$, quantifies the participation of the IBR at bus-k to the mode, and hence quantifies the involvement of the IBR in this interaction. For example, if the PLLs of several neighbouring IBRs are interacting with each other and result in a mode λ, the magnitude of their residues at λ, $\|\mathrm{Res}_{\lambda}^{*} Y_{kk}^{\mathrm{sys}}\|$, will be large. Consequently, according to (13), IMR_k will be small, representing a weak system seen from these POIs. In such a way, the interactions among IBRs are reflected in IMR.

From a more general perspective, whole-system admittance Y^{sys} is formed through a feedback arrangement of Y_{N} and Z_{A}, as introduced in III-A1. As a key feature, all elements in Y^{sys} contain dynamics of the whole-system, including all the controller interactions [20]. The IMR, which is defined through the element Y_{kk}^{sys}, then holds this property.

Property 3. *IMR is calculated at* $s = \lambda$. *When multiple oscillatory modes are observed at a location, the overall small-signal strength at bus-k is determined by the minimum IMR. When a mode is not observable at a POI, it is unnecessary, and indeed not possible, to calculate IMR of that mode at that POI.*

System oscillatory modes need to be identified before calculating IMR. Although a large-scale system would have a vast number of modes, it is unnecessary to calculate IMR for each of them. Only the most troublesome modes, i.e., those with small damping factors that may go on to cause oscillations need to be picked out to calculate the IMR. These modes are usually reflected as 'peaks' in the whole-system admittance spectrum. When no peaks can be identified in the whole-system admittance, it means this POI is not responsible for any of the oscillations that may occur in the system, thus is considered strong. It is also worth mentioning that high-frequency oscillations are usually well-damped by lines and do not readily spread across the system, so they are not considered important for this type of system strength assessment. As a result, the focus is on low-frequency modes, which further

simplifies the assessment process. In the reminader of this paper, only modes under 100 Hz are picked out for strength assessment.

Property 4. *IMR is dependent on the system operating point, the rating of the apparatus, and the apparatus control parameters.*

As a small-signal system strength metric, IMR would vary when the system operating point changes since the non-linear system will need to be re-linearised at the new operating point. This means that for practical application, it is recommended to estimate IMR at many credible operating points, or regularly in real-time. Moreover, the impedance value is dependent on the apparatus's rating and control parameters. By scaling up or scaling down the apparatus in power rating (more or fewer units in the farm), or by carefully tuning the control parameters, apparatus with small IMR would be able to create a ΔZ_{A} in the desired direction that can shift the mode leftward and improve damping. This property opens up a path towards an enhancement of system services: an IBR with the flexibility to change its impedance would be able to provide services to system operators to increase small-signal system strength.

It is also worth mentioning that IMR is based on a linearisation and the linearity is valid within a small range of the original operating point. This means that when IMR is small, it is a linear metric and the impedance margin is more accurate. On the contrary, a very large IMR does not necessarily mean that the impedance has a margin exactly the same as the calculated result, because of non-linear effects, but is still considered large. Nevertheless, only cases of small IMR need to be of concern for system strength management.

IV. Relationship with SCR

As a newly proposed system strength metric, it is important to clarify the relationship between it and the widely used SCR.

When a system is viewed from a single bus with an IBR connected, bus-k in this example, a linearisation can be made on the rest of the system to create an equivalent ideal voltage source in series with a Thévenin impedance $Z_{th,k}$, as shown in Fig. 3(a). When a three-phase short-circuit happens at bus-k, the power flows from the system to bus-k is defined as the short-circuit capacity (SCC), and is expressed as

$$\mathrm{SCC}_k = \frac{|V_s|^2}{|Z_{th,k}|} \tag{14}$$

SCR is then defined as the ratio between SCC and the nominal power of the device, P_{Nk}, connected to bus-k, i.e.,

$$\mathrm{SCR}_k = \frac{\mathrm{SCC}_k}{P_{Nk}}. \tag{15}$$

In a per unit system where the nominal voltage is 1 $p.u.$, SCR can be expressed in the following equation:

$$\mathrm{SCR}_k = \frac{1}{|Z_{th,k,pu}| \cdot P_{Nk,pu}} \tag{16}$$

For the sake of brevity, the per unit symbol will be omitted from the following discussion. A global base power is also chosen depending on the scale of the system.

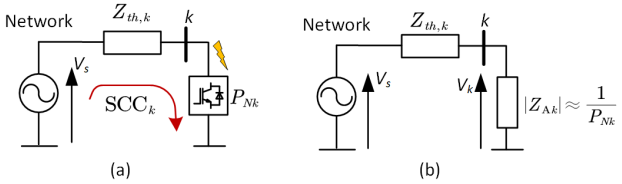


Fig. 3. Views of SCR: (a) from traditional short-circuit current view, and (b) from equivalent impedance view.

SCR can also be understood from a view that a negative load $Z_{\mathrm{A}k}$ is connected at bus-k. It has a negative real part and is sourcing active power with P_{Nk}, as shown in Fig. 3(b). The reactive power is assumed to be zero and the bus voltage V_k is assumed to be maintained close to 1. This assumption is reasonable because reactive power output of a grid-following IBR is usually considered very small to meet the grid code, and the magnitude of bus voltage is usually well-maintained. As a result, the magnitude of this impedance at base frequency can be approximated as

$$|Z_{\mathrm{A}k}| = \frac{|V_k|^2}{P_{Nk}} \approx \frac{1}{P_{Nk}}. \tag{17}$$

As a general rule of power flow analysis, voltage at bus-k will collapse when $|Z_{\mathrm{A}k}| < |Z_{th,k}|$. As a result, the Thévenin impedance of the system sets a minimum magnitude that $Z_{\mathrm{A}k}$ can have to avoid voltage collapse i.e.,

$$|Z_{th,k}| = |Z_{\mathrm{A}k}|_{\min}. \tag{18}$$

Substituting (17) and (18) into (16) yields

$$\mathrm{SCR} = \frac{|Z_{\mathrm{A}k}|}{|Z_{\mathrm{A}k}|_{\min}}, \tag{19}$$

i.e., SCR equals the ratio between the equivalent impedance of the device when delivering its nominal power and the minimum impedance that can be allowed to connect at that POI to maintain the voltage.

By increasing the nominal power of the apparatus, $Z_{\mathrm{A}k}$ will shrink to $Z'_{\mathrm{A}k}$ and maintain the same angle, as shown by the red arrow in Fig. 4. Once the magnitude shrinks to $|Z_{\mathrm{A}k}|_{\min}$, the impedance variation reaches to $|\Delta Z_{\mathrm{A}k}|_{\max}$, which sets the impedance margin and via (12) sets IMR. It can be seen from Fig. 4 that SCR represents a special case of IMR, in which the impedance margin is determined by the minimum allowed impedance to avoid voltage collapse rather than the margin toward mode instability. Note that in this case ΔZ is in the opposite direction to $Z_{\mathrm{A}k}$ rather than at an arbitrary direction. In this special case IMR < 1 and it follows from Fig. 4 that

$$\mathrm{SCR} = \frac{1}{1 - \mathrm{IMR}_0} \tag{20}$$

where we use IMR_0 to represent IMR evaluated at the base frequency value.

This discussion shows that there is some broad similarity between IMR and SCR but IMR is specifically defined in terms of small-signal system strength and the margin toward instability of an oscillatory mode whereas SCR addresses behaviour of voltage and current at fundamental frequency.

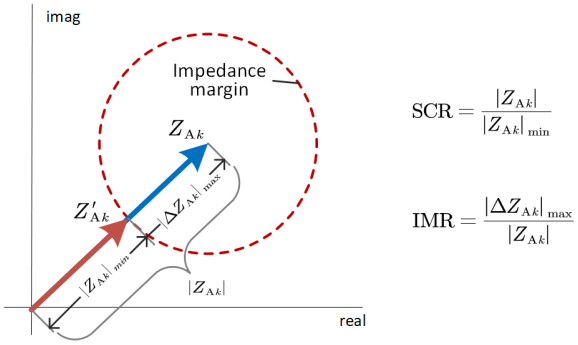


Fig. 4. Relationship between IMR and SCR: at the base frequency, the impedance margin is set by the minimum allowed impedance, i.e., the Thévenin impedance.

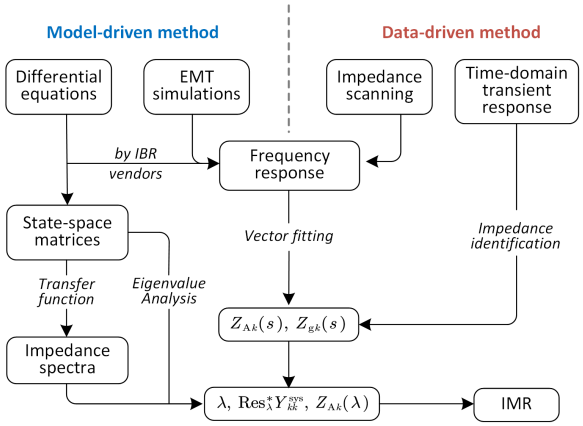


Fig. 5. Instructions for IMR practical implementations.

V. Approaches to Practical Implementation

A. Evaluation of IMR

To evaluate the IMR at each POI, according to (13), requires values of the terms σ, $\mathrm{Res}^*_\lambda Y^{\mathrm{sys}}_{kk}$ and $Z_{\mathrm{A}k}$. The first two can be extracted from Y^{sys}_{kk}. Equation (3) states that Y^{sys}_{kk} can be found from $Z_{\mathrm{g}k}$ and $Z_{\mathrm{A}k}$. In summary, at POI-k, the grid impedance $Z_{\mathrm{g}k}$ and the apparatus $Z_{\mathrm{A}k}$ are needed for the evaluation of IMR. Here are two essential methods to obtain IMR. Since impedance model is dependent on the operating point, it is recommended to estimate IMR at many credible operating points, or regularly in real-time.

1) Model-driven Method: This method is applicable when the IBR vendor is able to disclose the impedance model of the apparatus to the system operator, or alternatively, the system operator can share information of grid impedance with the IBR vendor. The impedance shared between the two parties can be either differential equations or numerical format.

If differential equations are used, linearisation needs to be performed around an operating point to obtain state-space matrices, which can then be transformed into impedance transfer functions. Impedance spectra can then be acquired by letting $s = j\omega$. The oscillatory mode can be known from the eigenvalue of the state-space matrix. This is the method used in the case studies in this paper.

In some cases, the shared model between vendors and operators could be frequency response data, i.e., impedance magnitude and angle at a set of frequency points [22]. Such frequency responses can be acquired either from an analytical model but shared in a discrete form for data-protection purposes, or obtained from the electromagnetic transient (EMT) simulation by using impedance analysis to avoid the need to form and manipulate differential equations. A vector fitting is usually needed [23] in this case. Values of σ (or more general, λ) and $\mathrm{Res}^*_\lambda Y^{\mathrm{sys}}_{kk}$ can be readily acquired from the results of vector fitting of $Y^{\mathrm{sys}}_{kk}(j\omega)$ data, and $Z_{\mathrm{A}k}(\lambda)$ can be extracted from the fitted result of $Z_{\mathrm{A}k}(j\omega)$. As mentioned when discussing IMR property 3, only the most troublesome modes are of concern, meaning that it is unnecessary to set a high order of approximation when performing vector fitting. [24] shows a case where 81 impedance frequency response points between 1 Hz to 1,000 Hz are applied for vector fitting data from a 14-bus system. It is found that with a 20^{th}-order approximation, $\mathrm{Res}^*_\lambda Y^{\mathrm{sys}}_{kk}$ and λ can be obtained with an accuracy over 99.8% compared with analytical results. Nevertheless, it is worth mentioning that impedance scanning in EMT simulation may be time-consuming.

2) Data-driven Method: The most straightforward approach to acquire impedance model from data is frequency scanning. It is reliant on injecting small voltage perturbations in the system and measuring the current response for admittance scanning, or injecting current and measuring voltage for impedance scanning. After acquiring the frequency response from an admittance scanning, the rest of the process is the same as the second case in the model-driven method. This method avoids any sharing of sensitive information but assesses system strength only based on the sampled data, hence we call it a data-driven method. When injection and measurement can be performed on-line [25], a real-time IMR assessment can also be performed to give early warning to system operators when 'weak areas' are spotted.

Recent research work also reveals that the impedance model can be identified from time-domain data of the transient period during events in the system, through system identification algorithms such as eigensystem realization algorithm (ERA) [26]. This method opens up a path of using time-domain data, such as data measured from a phasor measurement unit (PMU), to directly extract information of $Z_{\mathrm{A}}(s)$ and $Z_{\mathrm{g}}(s)$, which further derive IMR.

The data-driven approach is a promising approach for small-signal strength assessment as well as for root-cause tracing, and is especially suitable when white-box models are not made available. It can also address the dependency of impedance on the operating point because impedance is evaluated in real-time. Nonetheless, it is worth noting that additional hardware may be required for impedance scanning and high-bandwidth data sampling.

The above two methods for IMR practical implementation are summarised in Fig. 5.

B. Application of IMR

As a metric for small-signal system strength, IMR can be applied by system operators and IBR vendors in both planning

of IBR connections and during real-time operation.

1) IMR for System Planning: During the system planning stage where an apparatus is going to connect to the POI, the system operator can provide the grid impedance Z_{gk} in different scenarios, e.g., high-demand period, low-demand period, etc., to the apparatus vendor. The vendor, who has knowledge of the apparatus impedance Z_{Ak}, can then estimate IMR at different conditions, and ensure an acceptable IMR in different scenarios. If low IMR is spotted in some cases, the vendor will need to optimise its control and hardware design, or prepare plans for these cases such as curtailing its output power or purchasing services from other parties. Meanwhile, to verify the interaction of the new apparatus with the existing apparatus across the grid, the vendor could provide a black-box apparatus EMT model to the system operator, from which the system operator can acquire the frequency response data after connecting the apparatus to the grid in simulation, and further estimate IMR for various operating conditions. From the simulation results, the system operator can verify if the new apparatus can maintain a good IMR and whether will affect the IMR at other POIs across the network.

2) IMR for System Operation: IMR can also be estimated regularly in real-time. This process would be mainly performed by the system operator who is able to extract apparatus impedance and grid impedance through either impedance measuring equipment or through identification based on time-domain sampled data. By periodically assessing IMR at different locations, 'weak' areas can be spotted which can provide early warnings to system operators. At this time, efforts on validating the practicality of performing injections to the system for frequency scanning [25], analysis of measurement and sampling noise [27], as well as impedance identification through time-domain response are still ongoing [26].

VI. Case Studies

Two case studies have been performed to validate the performance of IMR. First, a 4-bus system is employed to illustrate the merits of the proposed IMR compared with existing metrics in describing the system strength in respect of oscillatory behaviour and IBR control interactions. Second, a modified IEEE 68-bus test system is used to demonstrate the application of IMR in a large-scale power system. The system data, the codes, and the models are available at [28].

A. 4-bus test system

A 4-bus system with one SG and two IBRs is established, as shown in Fig. 6. The per-unit values at the base frequency (50 Hz) of the components are marked in the figure, but it should be noted that the analysis is carried out in frequency domain. The two IBRs are configured as grid-following inverters equipped with PLL. Each IBR delivers 0.32 pu active power to the grid, which is also treated as their nominal power for SCR calculation. Three sub-cases are further studied.

1) case 1-a, baseline: The first case sets the baseline, where the two IBRs have identical control designs and are tuned well. SCR is first calculated at both POI-2 and POI-3 using (16). For the SCR calculation, the IBR and load are considered to have no fault contribution, i.e., they are treated disconnected when calculating SCR. The SG is treated as an ideal voltage source. For example, for POI-2, the Thévenin impedance is

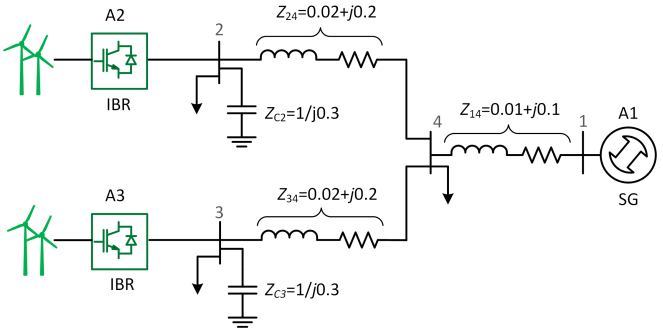


Fig. 6. Single-line diagram of the 4-bus test system with two IBRs and one SG. Line parameters are given in per unit value at the base frequency (50 Hz). Detailed system data is available in [28].

$$Z_{th,2} = (Z_{14} \parallel (Z_{34} + Z_{C3}) + Z_{24}) \parallel Z_{C2} = 0.037 + j0.333, \quad (21)$$

which further denotes the SCR

$$\text{SCR}_2 = \text{SCR}_3 = \frac{1}{|Z_{th,2}| \cdot P_{N2}} = 9.32. \quad (22)$$

According to [5], such a value of SCR represents a strong system.

Bode diagrams of Y_{22}^{sys} and Y_{33}^{sys} in d-d axis are further acquired and shown in Fig. 7(a). From the discussion in Section V, the bode diagram can be acquired from the state-space model if it is available, or from frequency response analysis in EMT simulations when only black-box models are available. In the case studies of this paper, results are derived from the analytical model, i.e., the state-space model. It can be noticed that there is a modest peak around 74 Hz, representing a mode of 74 Hz. From the transfer function, the exact mode and the corresponding residue can be extracted, and IMR can then be calculated at this mode using (13):

$$\lambda^{(1)} = -8.87 + j73.94 \text{ Hz}, \ \ \text{IMR}_2^{(1)} = \text{IMR}_3^{(1)} = 0.83, \quad (23)$$

where the superscript '(1)' represents the first sub-case. Such IMR value indicates that 83% of the change of the IBR impedance may possibly lead to the entire system being unstable. This is fairly accepted from a small-signal perspective. On the one hand, small perturbations are typically considered smaller than 83%, meaning the margin is enough. On the other hand, it means that there is still an oscillatory mode existed which may become worse along with system changes. In a time-domain simulation in which output power of A2 P_{out2} is increased by 25%, an approximate 74 Hz oscillation is observed in the voltage magnitude at POI-2 and POI-3, as shown in Fig. 7(d), but is decayed quickly. In this baseline, both SCR and IMR indicate a relatively strong system.

2) case 1-b, control interactions: This case aims to demonstrate the situation that IMR is able to capture the changes in the internal control of an IBR and interactions between IBRs, while SCR cannot. In this case, PLL of both the IBRs are deliberately detuned higher to 40 Hz, which is 4 times

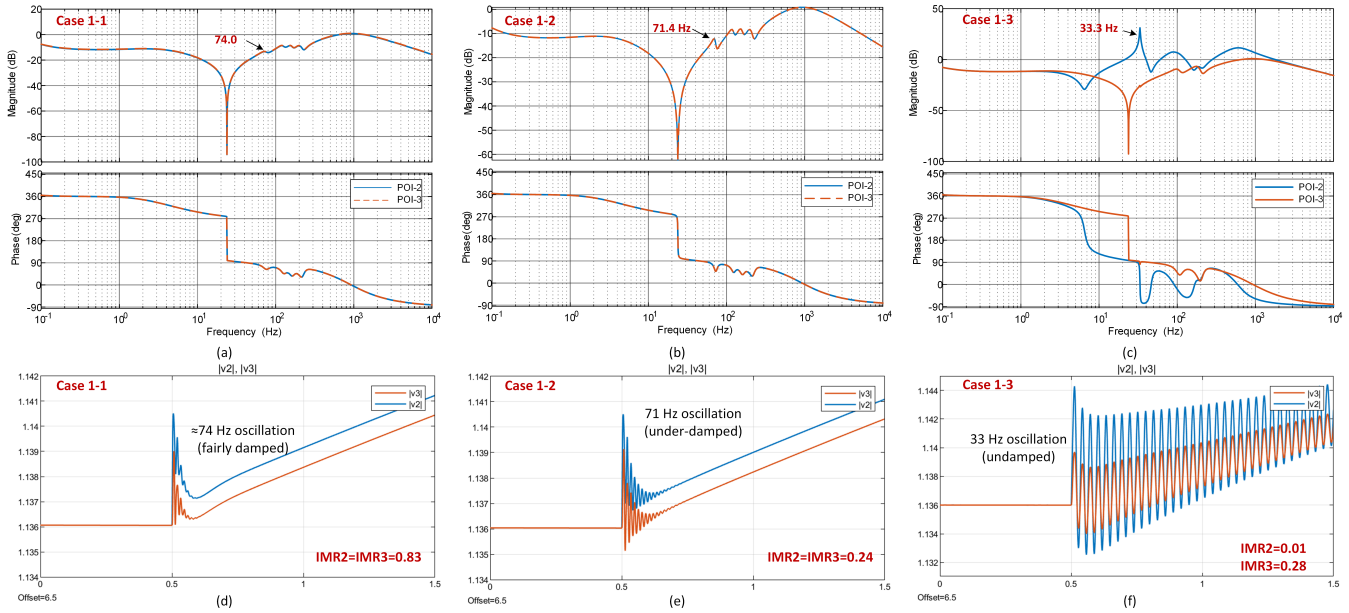


Fig. 7. (a)(b)(c) Bode diagram of Y_{22}^{sys} and Y_{33}^{sys} in d-d frame, in three different sub-cases. (d)(e)(f) Voltage magnitude of bus-2 and bus-3 when a 25% step increase of the output power of A2 is introduced at t=0.5 s.

the baseline value. The poor designs of A2 and A3 together lead to an oscillatory mode of 71.4 Hz, which stands out in the spectrum shown in Fig. 7(b). This implies that there is a control interaction between the two IBRs. Because the two IBRs have the same parameters, they are participating in this interaction equally. Since the network parameters remain the same, SCR at both POIs is still 9.32. The IMR value for this mode can be acquired using the same method in case 1-a, and the values are:

$$\lambda^{(2)} = -3.95 + j71.39 \text{ Hz}, \;\; \text{IMR}_2^{(2)} = \text{IMR}_3^{(2)} = 0.24. \quad (24)$$

It is noticeable that IMR values are dramatically decreased compared with the baseline, meaning that IMR can successfully capture the influence of the control interaction whereas the conventional SCR cannot. The observation from time-domain simulations given in Fig. 7(e) where an evident 71 Hz oscillation happened during the step change further proves such a fact.

3) case 1-c, localisation: This case aims to demonstrate the merit of IMR as a localised system strength metric. The two IBRs are tuned differently in this case: A2 has a PLL of 22 Hz and a current PI control bandwidth of 400 Hz, while A3 remains the same as the baseline: PLL of 10 Hz and current control bandwidth of 1500 Hz. Through the spectra in Fig. 7(c), a significant 33.3 Hz mode is identified on Y_{22}^{sys}. IMR of both IBRs are calculated at this mode:

$$\begin{aligned} \lambda^{(3)} &= -0.29 + j33.35 \text{ Hz} \\ \text{IMR}_2^{(3)} &= 0.01, \text{IMR}_3^{(3)} = 0.28. \end{aligned} \quad (25)$$

The results indicate that 1) POI-2 is much weaker than POI-3 due to its smaller IMR, and 2) both POIs become weaker compared with the baseline due to interactions of the controllers. The results of time-domain simulations are given in Fig. 7(f), which show that a series of poorly damped 33 Hz oscillations occur after the step change at P_{out2}. From time-domain response, or from small-signal gSCR [15] which uses a single number to describe the strength of the entire system, it is difficult to determine the oscillation liability. In contrast, the value of IMR reveals that IBR-2 should be considered responsible for driving the system to a very weak situation. IBR-3, despite is involved in the interaction and having a smaller IMR than before, should not be considered responsible for this oscillation. This is very useful for liability determination towards instabilities where several parties are involved: the IBR with the smallest IMR should take the primary responsibility. It should re-tune its parameters, pay for other system strength support services, or simply disconnect from the grid.

The control parameters and the results of the three sub-cases are summarised in the appendix in Table A1. Compared with conventional SCR, it is apparent that IMR can capture the change of IBR internal control design as well as control interactions whereas SCR cannot. Compared with other existing small-signal system strength metrics, IMR also shows prominent advantages. For example, compared with the grid strength impedance metric (GSIM) in [14] which is an entire frequency spectrum which needs to be interpreted, IMR is a single real number at each location with specific physical meaning, hence can support more straightforward rules for system strength assessment. Compared with small-signal gSCR [15] which uses a single value to represent the small-signal strength of the entire system (i.e. is not locational), the IMR values at locations across the system can help to identify the multiple weak areas in the system simultaneously, and also can help determine the liability for the IBR interaction.

According to (13), it is obvious that IMR=0 is the boundary of system being stable. However, the minimum required IMR

for robust system operation is not yet understood. Nevertheless, through a number of case studies with different parameters, we carefully list the following instructions which can be used as an initial guideline:

- IMR>0.5: system is strong. Changes in the configuration or operating point of apparatus at this location are unlikely to make the system unstable and poorly damped oscillations are unlikely to be observed at this location.
- IMR<0.5 and IMR>0.1: system is weak. Oscillations can be easily triggered and observed at this location. Careful attention must be paid to changes in the appratus at this location.
- IMR<0.1 and IMR>0: system is very weak. Changes at this location can easily cause significant and long-lasting oscillations and can propagate to the entire system. Immediate actions should be taken to increase the system strength.

This proposed guideline is based in part on the definition of IMR and in part on a limited number of case studies. More refined thresholds should be defined based on more experience obtained from simulations, commissioning, and field testing.

B. 68-bus system

To further validate the effectiveness of IMR in a large-scale composite system, a modified IEEE 68-bus system with 14 extra IBR configured as grid-following inverters was created, as shown in Fig. 8.

IMR is then evaluated at each bus where an IBR is connected. If more than one mode is observable at a bus, the minimum IMR is taken as the overall indicator of the small-signal strength at that location. Three sub-cases are created and an IMR heatmap is plotted for each case, as shown in Fig. 9. In case 2-a, all IBRs are properly tuned to enable the system to work in a stable manner, with their parameters chosen in a reasonable range. The IMR heatmap in Fig. 9(a) indicates that all areas maintain an IMR above 1, indicating a healthy small-signal strength at all locations. In case 2-b, all IBRs except A58 and A59 are deliberately detuned by increasing their base power, increasing the phase-lock loop (PLL) bandwidth and decreasing the current control bandwidth. The detuning levels on each IBR differ from each other to represent a system with multiple IBR vendors and designs but all with the same trend of poor tuning. It is expected that such detuning will lower the system strength at the detuned locations and lead to greater oscillatory behaviour. From the IMR heatmap shown in Fig. 9(b), it can be observed that the IMR in the region of buses 26, 28, 29, and the region of buses 35, 39, 43, 44, 45, 50, 51 is significantly decreased, noted as their color being yellow. This indicates a weak system seen from these locations, whereas IMR at buses 58 and 59 remains at a high level, implying a strong system in this region. In case 2-c, IBRs excluding A58 and A59 are further detuned following the same trend in case 2-b. It is expected that the system will become very weak at the detuned areas but will still remain strong at buses 58 and 59. Such a situation is also successfully indicated by the IMR heatmap, as shown in Fig. 9(c).

A set of EMT simulations is then performed to validate the results shown in IMR heatmaps. At $t = 6\ s$, a 25% step-increase of the loads at buses 28, 39 and 59 is introduced, and voltage magnitudes at these buses are taken for comparisons, as shown in Fig. 10. It is evident that the oscillations during the step-change become more significant when IMR is indicating a weaker system.

Fig. 11 shows the Bode diagram of Y_{kk}^{sys} in case 2-c at POIs with IBR connected . From the spectra, it can be noticed that a significant 24 Hz peak appeared on the spectra at POI-39, 44, 45 and nearby locations, and 28 Hz and 87 Hz peaks appeared on the spectra at POI-28, 29, 26. Such results reveal that areas near POI-39 and POI-28 are weak and oscillations may occur following perturbations in the system. It is also noted that admittance spectra at POI-58, 59 have nearly no peaks, indicating that this area is strong. The observations from the bode plot align with the results in the IMR heatmap and time-domain simulation. The exact values of IMR at different POI in different sub-cases are provided in Table A2 in the appendix.

This case study proves that IMR can be applied in a large-scale composite system. With the help of an IMR heatmap, system operators can efficiently identify the locations where oscillations are easier to be triggered and get early warnings for system risks.

VII. Conclusions

This paper first draws a distinction between small-signal system strength and large-signal system strength which is a natural separation considering the distinctly different response of an IBR in normal operation and under faults. Impedance margin ratio (IMR) is then proposed as a new metric for small-signal system strength. It is defined as the ratio between the allowed change in IBR impedance and its original impedance value at the frequency of oscillation of a mode of concern. The allowed change in IBR impedance is set, in a conservative fashion, in terms of avoiding causing the mode to move to the right half plane. IMR is shown to have a relationship with the conventional system strength metric, SCR, but is different in not being restricted to fundamental frequency impedance. Practical routes to computing IMR from either a state-space system model or from impedance data obtained from measurement or EMT simulation have been discussed. It is proved through case studies that IMR is a metric that successfully identifies system response towards small disturbances and onset of oscillatory behaviour. Initial studies find that an IMR smaller than 0.5 indicates a weak system. Through an IMR heatmap, system operators can readily identify the weak areas in the system and can take early measures to reduce risks of oscillation.

Appendix A
Case Studies

System data and IMR results for the 4-bus system are given in Table A1. The IMR results of the modified IEEE 68-bus system are given in Table A2.

References

[1] IEA, "Global Energy Review 2021," Accessed: Feb. 20, 2024. [Online]. Available: https://www.iea.org/reports/global-energy-review-2021/renewables

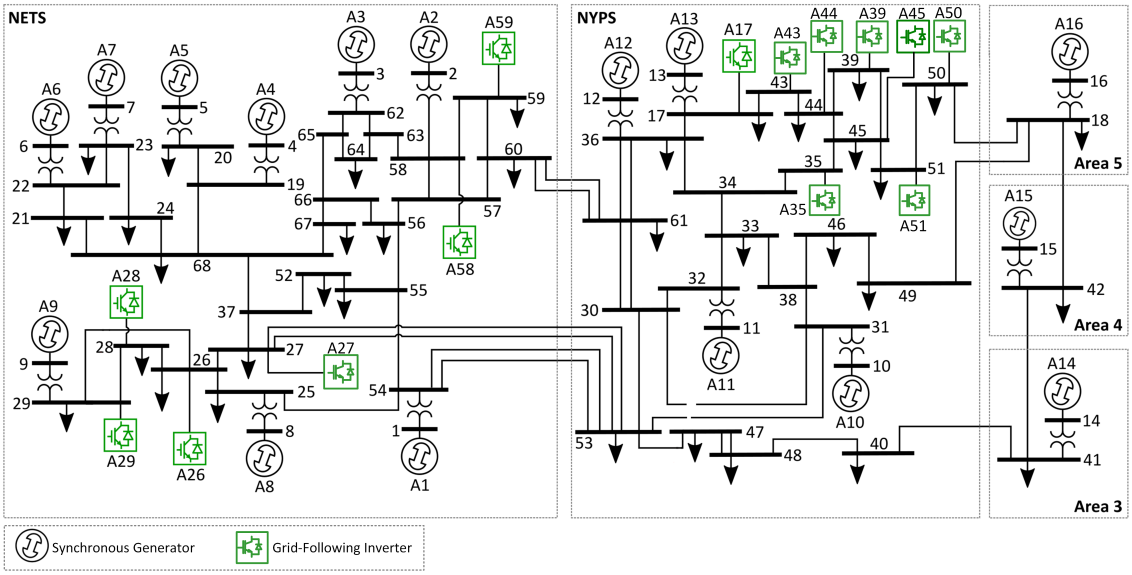


Fig. 8. Single-line diagram of the modified IEEE 68-bus system: 14 additional grid-following inverters are added in different buses. Detailed system data is available in [28].

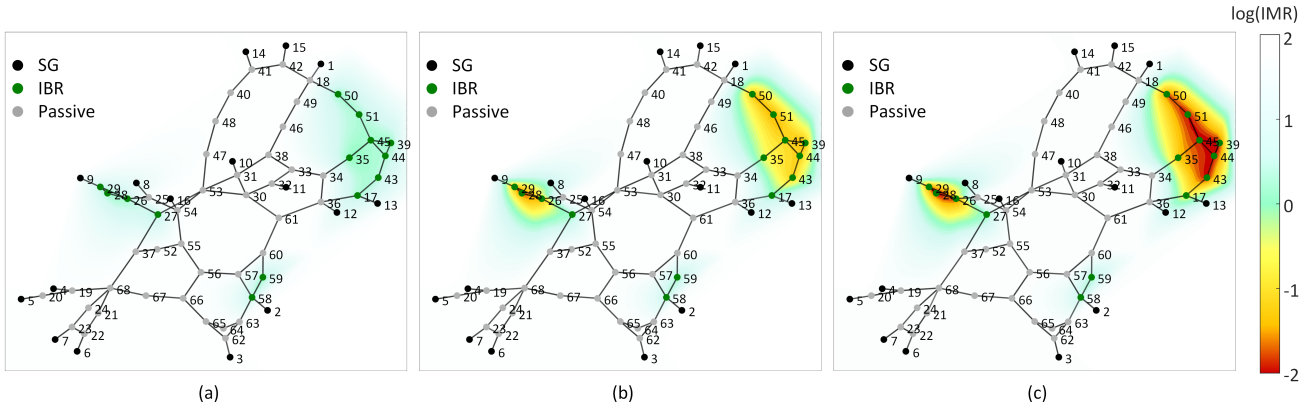


Fig. 9. IMR heatmap of the modified 68-bus system: (a) all IBRs are properly tuned. (b) IBRs except A58 and A59 are deliberately detuned to different levels. (c) IBRs except A58 and A59 are further deliberately detuned. The common logarithm of IMR is applied to distribute the color bar in an even fashion. The IMR heatmap correctly shows the trend of the detuning and quickly exposes areas with low strength.

TABLE A1
CONTROL PARAMETERS AND IMR, SCR RESULTS FOR THE 4-BUS TEST SYSTEM CASE STUDIES

		PLL Bandwidth	Current PI Bandwidth	IMR	SCR
1-a	IBR2	10 Hz	1500 Hz	0.83	9.32
	IBR3	10 Hz	1500 Hz	0.83	9.32
1-b	IBR2	40 Hz	1500 Hz	0.24	9.32
	IBR3	40 Hz	1500 Hz	0.24	9.32
1-c	IBR2	22 Hz	400 Hz	0.01	9.32
	IBR3	10 Hz	1500 Hz	0.28	9.32

TABLE A2
IMR RESULTS FOR THE 68-BUS TEST SYSTEM CASE STUDIES

Bus	2-a	2-b	2-c	Bus	2-a	2-b	2-c
17	1.674	1.463	0.230	43	2.229	0.077	0.005
26	1.412	0.043	0.014	44	2.163	0.074	0.009
27	1.782	1.228	1.001	45	1.790	0.102	0.013
28	1.386	0.016	0.006	50	1.249	0.046	0.017
29	1.700	0.020	0.007	51	1.841	0.036	0.010
35	1.018	0.352	0.059	58	1.920	2.264	2.264
39	1.135	0.044	0.004	59	1.550	1.849	1.853

[2] Y. Li, Y. Gu, and T. C. Green, "Interpreting frame transformations in ac systems as diagonalization of harmonic transfer functions," *IEEE Transactions on Circuits and Systems I: Regular Papers*, vol. 67, no. 7, pp. 2481–2491, 2020.

[3] Y. Gu, J. Liu, T. C. Green, W. Li, and X. He, "Motion-induction compensation to mitigate sub-synchronous oscillation in wind farms," *IEEE Transactions on Sustainable Energy*, vol. 11, no. 3, pp. 1247–1256, 2019.

[4] Y. Gu and T. C. Green, "Power system stability with a high penetration of inverter-based resources," *Proceedings of the IEEE*, vol. 111, no. 7, pp. 832–853, 2023.

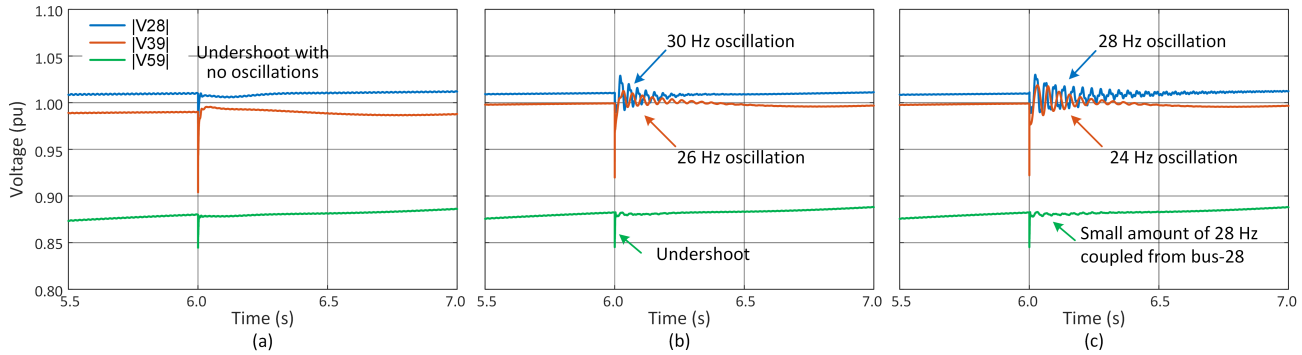


Fig. 10. Voltage magnitude of bus-28, 39 and 59 during a 25% step increase of the loads at these buses: (a) all IBRs are properly tuned, showing no oscillations. (b) IBRs except A58 and A59 are deliberately detuned, showing significant oscillations. (c) IBRs except A58 and A59 are further deliberately detuned, showing even worse oscillations. The time-domain results verify what has been revealed in the IMR heatmap.

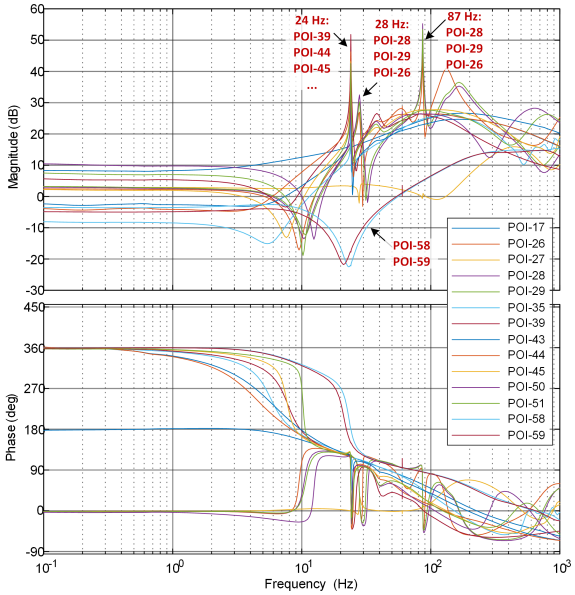


Fig. 11. Bode diagram of whole-system admittance at POI with IBR connected in case 2-c, in *d-d* frame.

[5] CIGRE, "Connection of Wind Farms to Weak AC Networks," 2016, Accessed: Feb. 20, 2024. [Online]. Available: https://e-cigre.org/publication/671-connection-of-wind-farms-to-weak-ac-networks

[6] B. Badrzadeh, Z. Emin *et al.*, "System strength," *CIGRE SCIENCE & ENGINEERING*, vol. N20, pp. 5–27, 2021.

[7] S. Gordon, K. Bell, and Q. Hong, "Implications of reduced fault level and its relationship to system strength: A scotland case study," *CIGRE Session 2022*, 2022.

[8] National Grid ESO, "Provision of Short Circuit Level Data," 2022, Accessed: Feb. 20, 2024. [Online]. Available: https://www.nationalgrideso.com/document/238741/download

[9] F. Zhang, H. Xin, D. Wu, Z. Wang, and D. Gan, "Assessing strength of multi-infeed lcc-hvdc systems using generalized short-circuit ratio," *IEEE Transactions on Power Systems*, vol. 34, no. 1, pp. 467–480, 2018.

[10] Australian Energy Market Commission (AEMC), "National Electricity Amendment (Managing power system fault levels) Rule 2017," 2017, Accessed: Feb. 20, 2024. [Online]. Available: https://www.aemc.gov.au/sites/default/files/content/4645acea-e66f-4b5b-94a1-1dd14e7f8a93/ERC0211-Final-determination.pdf

[11] A. Boričić, J. L. R. Torres, and M. Popov, "System strength: Classification, evaluation methods, and emerging challenges in IBR-dominated grids," *2022 IEEE PES Innovative Smart Grid Technologies-Asia (ISGT Asia)*, pp. 185–189, 2022.

[12] GE and MISO, "GE Energy Consulting: Minnesota Renewable Energy Integration and Transmission Study (Final Report)," 2014, Accessed: Feb. 20, 2024. [Online]. Available: http://mn.gov/commerce-stat/pdfs/mrits-report-2014.pdf

[13] Y. Zhang, S.-H. F. Huang, J. Schmall, J. Conto, J. Billo, and E. Rehman, "Evaluating system strength for large-scale wind plant integration," in *2014 IEEE PES General Meeting| Conference & Exposition*. IEEE, 2014, pp. 1–5.

[14] C. Henderson, A. Egea-Alvarez, T. Kneuppel, G. Yang, and L. Xu, "Grid strength impedance metric: An alternative to scr for evaluating system strength in converter dominated systems," *IEEE Transactions on Power Delivery*, pp. 1–10, 2023.

[15] W. Dong, H. Xin, D. Wu, and L. Huang, "Small signal stability analysis of multi-infeed power electronic systems based on grid strength assessment," *IEEE Transactions on Power Systems*, vol. 34, no. 2, pp. 1393–1403, 2019.

[16] F. Ma, H. Xin, D. Wu, Y. Liu, and X. Chen, "Assessing grid strength of 100% inverter-based power systems," *TechRxiv*, 2023. [Online]. Available: http://dx.doi.org/10.36227/techrxiv.21120517.v6

[17] Y. Zhu, Y. Gu, Y. Li, and T. C. Green, "Participation analysis in impedance models: The grey-box approach for power system stability," *IEEE Transactions on Power Systems*, vol. 37, no. 1, pp. 343–353, 2022.

[18] H. Gu, R. Yan, T. K. Saha, and E. Muljadi, "System strength and inertia constrained optimal generator dispatch under high renewable penetration," *IEEE Transactions on Sustainable Energy*, vol. 11, no. 4, pp. 2392–2406, 2020.

[19] Y. Gu, Y. Li, Y. Zhu, and T. C. Green, "Impedance-based whole-system modeling for a composite grid via embedding of frame dynamics," *IEEE Transactions on Power Systems*, vol. 36, no. 1, pp. 336–345, 2021.

[20] Y. Zhu, Y. Gu, Y. Li, and T. Green, "Impedance-based root-cause analysis: Comparative study of impedance models and calculation of eigenvalue sensitivity," *IEEE Transactions on Power Systems*, pp. 1–1, 2022.

[21] Y. Zhan, X. Xie, and Y. Wang, "Impedance network model based modal observability and controllability analysis for renewable integrated power systems," *IEEE Transactions on Power Delivery*, vol. 36, no. 4, pp. 2025–2034, 2021.

[22] D. Yang, X. Wang, M. Ndreco, W. Winter, R. Juhlin, and A. Krontiris, "Automation of impedance measurement for harmonic stability assessment of mmc-hvdc systems," in *18th Wind Integration Workshop*, 2019.

[23] B. Gustavsen and A. Semlyen, "Rational approximation of frequency domain responses by vector fitting," *IEEE Transactions on Power Delivery*, vol. 14, no. 3, pp. 1052–1061, 1999.

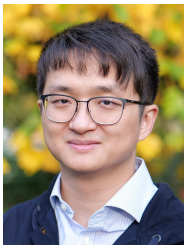
[24] Y. Zhu, "Impedance model analysis and measurement for power system stability," Ph.D. dissertation, Imperial College London, 2022.

[25] S. Shah, P. Koralewicz, R. Wallen, and V. Gevorgian, "Impedance characterization of utility-scale renewable energy and storage systems," in *2019 IEEE Energy Conversion Congress and Exposition (ECCE)*, 2019, pp. 2609–2616.

[26] L. Fan and Z. Miao, "Time-domain measurement-based DQ-frame admittance model identification for inverter-based resources," *IEEE Transactions on Power Systems*, vol. 36, no. 3, pp. 2211–2221, 2021.

[27] Y. Zhu, Y. Zhang, and T. C. Green, "Injection amplitude guidance for impedance measurement in power systems," *IEEE Transactions on Power Electronics*, vol. 38, no. 6, pp. 6929–6933, 2023.

[28] "Future power networks," Accessed: Feb. 20, 2024. [Online]. Available: https://github.com/Future-Power-Networks/Publications



Yue Zhu (S'19-M'22) received the B.Eng and M.Sc degrees in electrical engineering, Zhejiang University, Hangzhou, China, in 2016 and 2019 respectively. He received his Ph.D. degree in 2022 from Imperial College London, UK and is now a Post-Doctoral Research Associate at Imperial College London supported by National Grid ESO. His research focuses on impedance-based stability analysis of power systems, data-led impedance identification technology and analysis of system strength for inverter connection assessment.



Timothy C Green (F'19) received a B.Sc. (Eng) (first class honours) from Imperial College London, UK in 1986 and a Ph.D. from Heriot-Watt University, Edinburgh, UK in 1990. He is a Professor of Electrical Power Engineering and Academic Lead for Sustainability at Imperial College London. He was previously Director of the Energy Futures Lab with a role of fostering interdisciplinary research across the university. His research focuses on the role of power electronics in future power systems with very high fractions of renewable energy. In HVDC, he has contributed converter designs that strike improved trade-offs between power losses, physical size and fault handling. In distribution systems, he has pioneered the use of soft open points for relieving constraints in distribution networks. He has made important contribution to the study of stability of grids dominated by inverter-based resources. Prof. Green chairs the Engineering Advisory Council of National Grid ESO and is a member of the Advisory Council of the Electric Power Research Institute. He is a Chartered Engineering in the UK and a Fellow of the Royal Academy of Engineering and a Fellow of the Learned Society of Wales.



Xiaoyao Zhou received his bachelor and master degree from HoHai University, China in 1996 and 1999, respectively. He received his Phd in Electrical Engineering from Bath University, UK in 2006.

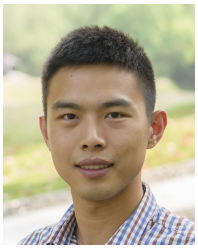
He joined National Grid since 2006 and has worked in transmission system operation, planning and investment. His current role is to set out operability policy for Great Britain's electricity network to enable the net zero operation, specify the Grid Code technical requirements for new technologies and define future network needs so that market and network owners can invest in the right solutions at the right time. He is also an Honorary Professor in University of Birmingham, UK.



Yitong Li (S'17-M'21) received the B.Eng degrees in electrical engineering from Huazhong University of Science and Technology, China, and the University of Birmingham, UK, in 2015. He received the M.Sc degree in future power networks and the Ph.D. degree in electrical engineering from Imperial College London, UK, in 2016 and 2021 respectively. He is currently a Professor at Xi'an Jiaotong University, China. His current research interests include control of power electronic converters and analysis of power system dynamics.



Dechao Kong received Ph.D degree from the University of Birmingham, Birmingham, UK in 2013. From 2020 to 2023, he worked for National Grid Electricity System Operator (ESO), UK as a Specialist Engineer with Subject-Matter Expertise in DC Systems and Power Electronics as well as Project Lead for ESO's Network Innovation Allowance Project – Strength to Connect. Dechao has been getting heavily involved in the UK's academia and industry for DC systems and Power Electronics since 2008, contributing his such subject-matter expertise in technical strategy & policy development, new technology & innovation, engineering and asset management. He is a Chartered Engineer and an elected IET Fellow in the UK.



Yunjie Gu (M'18-SM'20) received the B.Sc. and the Ph.D. degree in Electrical Engineering from Zhejiang University, Hangzhou, China, in 2010 and 2015 respectively. He is now a Lecturer at Imperial College London, where he was an EPSRC funded Innovation Fellow (award EP/S000909/1). Before his academic career, he was a Consulting Engineer at General Electric Global Research Centre, Shanghai, China. His research interests include stability theory for inverter-based power systems, stability-enhancing inverter technologies, and numerical methods for computer-aided stability analysis.